Modulation instability in amplitude modulated dispersion oscillating fibers

François Copie, Alexandre Kudlinski, Gilbert Martinelli, Arnaud Mussot, Matteo Conforti

Modulation instability in amplitude modulated dispersion oscillating fibers

François Copie,* Alexandre Kudlinski, Matteo Conforti, Gilbert Martinelli, and Arnaud Mussot

Laboratoire PhLAM, UMR CNRS 8523, IRCICA, USR CNRS 3380, Université Lille 1, 59655 Villeneuve dAscq, France

*francois.copie@univ-lille1.fr

Abstract: We investigate theoretically and experimentally the modulation instability process in a dispersion oscillating fiber characterized by an amplitude modulation of its group velocity dispersion. We developed an analytical model that allows us to calculate the parametric gain in these fibers and to predict the position of the quasi-phase matched modulation instability sidelobes. The two fundamental frequencies characterizing the dispersion profile lead to the splitting of the original multiple sidelobes generated in basic sinusoidally varying dispersion oscillating fibers. These theoretical predictions are confirmed by experiments.

OCIS codes: (190.4410) Nonlinear optics, parametric processes; (190.4380) Nonlinear optics, four-wave mixing; (190.4975) Parametric processes; (190.4223) Nonlinear wave mixing.

References and links

1. E. A. Golovchenko and A. N. Pilipetskii, "Unified analysis of four-photon mixing, modulational instability, and stimulated Raman scattering under various polarization conditions in fibers," J. Opt. Soc. Am. B **11**(1), 92–101 (1994).
2. R. H. Stolen and J. E. Bjorkholm, "Parametric amplification and frequency conversion in optical fibers," IEEE J. Quantum. Electron **18**(7), 1062–1072 (1982).
3. A. Kudlinski, A. Bendahmane, D. Labat, S. Virally, R. T. Murray, E. J. R. Kelleher, and A. Mussot, "Simultaneous scalar and cross-phase modulation instabilities in highly birefringent photonic crystal fiber," Opt. Express **21**(7), 8437–8443 (2013).
4. S. Pitois and G. Millot, "Experimental observation of a new modulational instability spectral window induced by fourth-order dispersion in a normally dispersive single-mode optical fiber," Opt. Commun. **226**(1–6), 415–422 (2003).
5. J. D. Harvey, R. Leonhardt, S. Coen, G. K. L. Wong, J. C. Knight, W. J. Wadsworth, and P. St. J. Russel, "Scalar modulation instability in the normal dispersion regime by use of a photonic crystal fiber," Opt. Lett. **28**(22), 2225–2227 (2003).
6. F. Matera, A. Mecozzi, M. Romagnoli, and M. Settembre, "Sideband instability induced by periodic power variation in long-distance fiber links," Opt. Lett. **18**(18), 1499–1501 (1993).
7. N. J. Smith and N. J. Doran, "Modulational instabilities in fibers with periodic dispersion management," Opt. Lett. **21**(8), 570–572 (1996).
8. F. K. Abdullaev, S. A. Darmanyan, A. Kobyakov, and F. Lederer, "Modulational instability in optical fibers with variable dispersion," Phys. Lett. A **220**(4–5), 213–218 (1996).
9. M. Droques, A. Kudlinski, G. Bouwmans, G. Martinelli, and A. Mussot, "Experimental demonstration of modulation instability in an optical fiber with a periodic dispersion landscape," Opt. Lett. **37**(23), 4832–4834 (2012).
10. M. Droques, A. Kudlinski, G. Bouwmans, G. Martinelli, and A. Mussot, "Dynamics of the modulation instability spectrum in optical fibers with oscillating dispersion," Phys. Rev. A **87**(1), 013813 (2013).
11. M. Droques, A. Kudlinski, G. Bouwmans, G. Martinelli, A. Mussot, A. Armaroli, and F. Biancalana, "Fourth-order dispersion mediated modulation instability in dispersion oscillating fibers," Opt. Lett. **38**(17), 3464–3467 (2013).

#228256 - $15.00 USD Received 20 Nov 2014; revised 9 Jan 2015; accepted 13 Jan 2015; published 9 Feb 2015

12. C. Finot, F. Feng, Y. Chembo, and S. Wabnitz, "Gain sideband splitting in dispersion oscillating fibers," Opt. Fiber Tech. **20**(5), 513–519 (2014).
13. A. Armaroli and F. Biancalana, "Vector modulational instability induced by parametric resonance in periodically tapered highly birefringent optical fibers," Phys. Rev. A **87**(6), 063848 (2013).
14. X. Wang, D. Bigourd, A. Kudlinski, K. K. Y. Wong, M. Douay, L. Bigot, A. Lerouge, Y. Quiquempois, and A. Mussot, "Correlation between multiple modulation instability side lobes in dispersion oscillating fiber," Opt. Lett. **39**(7), 1881–1884 (2014).
15. S. Trillo and S. Wabnitz, "Dynamics of the nonlinear modulational instability in optical fibers," Opt. Lett. **16**(13), 986–988 (1991).
16. G. Agrawal, *Nonlinear Fiber Optics*, 5th ed. (Academic , 2013).
17. M. E. Marhic, F. S. Yang, M. Ho, and L. G. Kazovsky, "High-nonlinearity fiber optical parametric amplifier with periodic dispersion compensation," J. Lightwave Technol. **17**(2), 210–215 (1999).
18. K. Saitoh and M. Koshiba, "Empirical relations for simple design of photonic crystal fibers," Opt. Express **13**(1), 267–274 (2005).

1. Introduction

Modulation instability (MI) is a nonlinear phenomena in which a weak perturbation of a continuous wave (CW) grows exponentially as a result of the interplay between dispersion and nonlinearity. It can also be interpreted in terms of a phase matched four-wave mixing (FWM) process [1]. Basically, a negative linear phase mismatch value must exist to compensate for the positive nonlinear one. In uniform single-mode optical fibers, considering a single polarization state, this can only be achieved in the anomalous dispersion regime where the group velocity dispersion is negative. In the normal dispersion regime, a perfect phase matching relation is only possible if an additional degree of freedom is provided, such as another spatial [2] or vectorial mode [3], or by working so close to the zero dispersion wavelength (ZDW) of the fiber that higher order dispersion terms must be accounted for [4, 5]. Another solution is to add a longitudinal periodicity to the system as it was theoretically investigated by Matera *et al.* in the context of telecommunication systems where the periodic variation of the power leads to the generation of multiple quasi-phase matched MI sidelobes [6]. The same behaviour was expected to occur in dispersion managed fibers [7, 8], and it was recently experimentally confirmed by Droques *et al.* who reported the generation of more than 10 pairs of quasi-phase matched MI sidebands in a photonic crystal fiber (PCF) in which the GVD was sinusoidally modulated [9]. Following this work, many investigations had been performed with this kind of dispersion oscillating fibers (DOFs) following a sine modulation, for instance, to find a simple analytical model of the parametric gain [10], to study the behaviour in the low dispersion regime [11], to consider the case of large amplitude of modulation [12], to enlarge the investigations to the vectorial case [13] or to investigate the correlation in energy between the sidelobes [14]. Except in [8] where a theoretical study of a random modulation of the GVD has been performed, all these investigations have been limited to a simple sinusoidal modulation of the dispersion.

In this work, we investigate the MI process in a much more complex configuration where the GVD of the fiber is amplitude modulated. The two distinct frequencies (related to oscillation and modulation periods) characterizing this modulation format dramatically modify the dynamics of the system leading to the appearance of new and unexpected MI sidelobes. We develop an analytical model to establish an expression for the parametric gain and for a specific quasi-phase matched relation which allows us to predict their position. Then, we investigate more deeply the dynamics of the system, namely the impact of the ratio between the periods of oscillation on the shape of the gain spectrum. Finally, we realize an experiment which confirms these theoretical predictions.

#228256 - $15.00 USD Received 20 Nov 2014; revised 9 Jan 2015; accepted 13 Jan 2015; published 9 Feb 2015

2. Analytical model

We follow the same procedure as the one developed in [10] to investigate sinusoidally varying DOFs. We remind the reader that the starting point of this development is a simplified truncated three-wave model that describes the MI process [15] when the phase matching relation evolves longitudinally. Starting from the three-wave model of MI, we assume that the fiber losses are negligible, the pump is undepleted and the signal and idler powers (P_s and P_i) remain weak compared to the pump power (P_p) along the fiber length. It leads to the following system of Eqs. [10]:

$$\frac{dP_s(\Omega,z)}{dz} = 2\gamma P_p \sqrt{P_s(\Omega,z)P_i(\Omega,z)}\sin[\theta(\Omega,z)] \tag{1}$$

$$\frac{dP_i(\Omega,z)}{dz} = 2\gamma P_p \sqrt{P_s(\Omega,z)P_i(\Omega,z)}\sin[\theta(\Omega,z)] \tag{2}$$

$$\frac{d\theta(\Omega,z)}{dz} = \beta_2(z)\Omega^2 + 2\gamma P_p\{1+\cos[\theta(\Omega,z)]\} \tag{3}$$

where γ is the nonlinear coefficient of the fiber, Ω is the pulsation shift of the signal and idler from the pump and $\theta(\Omega,z)$ expresses the relative phases between these three waves.

This model explicitly depends on the longitudinal variations of the group velocity dispersion (GVD, $\beta_2(z)$). In this work, rather than a basic sinusoidally modulated dispersion format we consider the following amplitude modulated profile:

$$\beta_2(z) = \bar{\beta_2} + \beta_2^A \sin\left(\frac{2\pi z}{Z_1}\right)\cos\left(\frac{2\pi z}{Z_2}\right) \tag{4}$$

where Z_1 is referred to as the oscillation period (short oscillation) and Z_2 the modulation period (long oscillation) of the GVD. An illustration of this profile is shown in Fig. 1(a) for $Z_1 = 5$ m and $Z_2 = 50$ m. In order to obtain a simple analytical solution, we neglect the term $\cos[\theta(\Omega,z)]$ in (3) which physically means that we assume that the longitudinal evolution of the nonlinear phase mismatch is weak compared to the linear and uniform nonlinear phase mismatches. We checked that this assumption is valid for a wide range of realistic parameters. After straightforward calculations, the signal gain in power reads as :

$$G_S(\Omega,z) = \frac{P_s(\Omega,z)}{P_s(\Omega,0)} = \frac{1}{4}(1-\rho) + \frac{1}{4}(1+\rho+2\sqrt{\rho})\exp[\int_0^z g(\Omega,\theta,z')dz'] \tag{5}$$

where $\rho = P_i(\Omega,0)/P_s(\Omega,0) = 1$ for the sake of simplicity and $g(\Omega,\theta,z) = 2\gamma P_p \sin[\theta(\Omega,z)]$ is the local linear gain. By integrating the system of Eqs. with our amplitude modulated GVD profile (4) and use of a Bessel series expansion, we find the following expression for the linear gain of an amplitude modulated fiber:

$$g(\Omega,z) = 2\gamma P_p \sum_{q=-\infty}^{+\infty}\sum_{q'=-\infty}^{+\infty} J_q\left(\frac{\beta_2^A\Omega^2}{2\Lambda_s}\right) J_{q'}\left(\frac{\beta_2^A\Omega^2}{2\Lambda_d}\right)\sin[(\Omega^2\bar{\beta}_2 + 2\gamma P_p - q\Lambda_s - q'\Lambda_d)z + \theta(0)] \tag{6}$$

with $\Lambda_s = 2\pi(Z_2+Z_1)/Z_1Z_2$, $\Lambda_d = 2\pi(Z_2-Z_1)/Z_1Z_2$ and $\theta(0)$ the initial relative phase sets to $\frac{\pi}{2}$. For a given detuning Ω, the linear gain is the sum of longitudinal sine functions with zero average values except for discrete spectral components for which the argument of the sine function is independent of z. These detunings are given by

$$\bar{\beta}_2\Omega_{kk'}^2 + 2\gamma P_p = k\Lambda_s + k'\Lambda_d \tag{7}$$

#228256 - $15.00 USD Received 20 Nov 2014; revised 9 Jan 2015; accepted 13 Jan 2015; published 9 Feb 2015

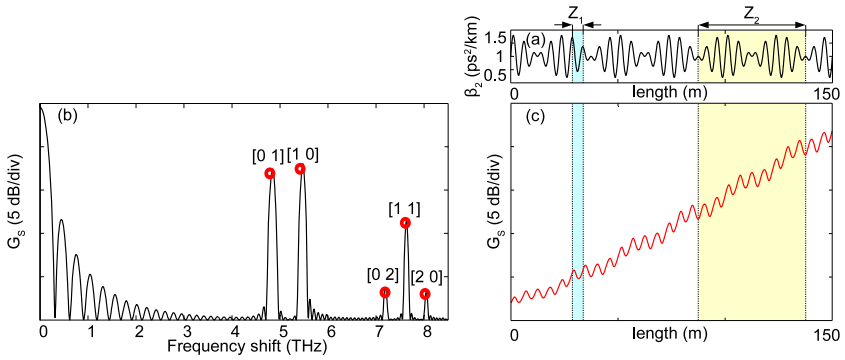

Fig. 1. (a) Typical amplitude modulated dispersion profile. (b) Corresponding gain spectrum simulated according to the NLS equation. The red circles represent the positions and maximum gain values of the sidelobes predicted by the analytical model. Each sidelobe is identified by its $[k\ k']$ label. (c) Longitudinal evolution of the gain of the first sidelobe calculated using the analytical model. A movie (Media 1) showing the evolution of the gain spectrum along the fiber length can be seen online. $L = 150$ m, $Z_1 = 5$ m, $Z_2 = 50$ m, $P_p = 15$ W, $\gamma = 7.5$ W^{-1}·km^{-1}, $\beta_2 = 1$ ps^2/km, $\beta_2^A = 0.8$ ps^2/km.

which can be interpreted as a quasi-phase matching relation where the right-hand side terms constitute the contribution of the amplitude modulated dispersion grating. For these detunings, the waves are quasi-phase matched, leading to the amplification of the signal and idler waves. Equations (7) and (6) can then be used to predict the positions and maximum gain values of the sidelobes in amplitude modulated DOFs. We can label each sidelobes by the pair of indices $[k\ k']$ (with k and k' integers) corresponding to the term in Eq. (6) giving rise to a gain of amplification.

To validate our analytical model, its predictions are compared to numerical simulations performed by integrating the Nonlinear Schrödinger equation (NLSE) [16] using a split-step Fourier method with a monochromatic seed scanning over the frequency range in order to measure the gain. Red circles in Fig. 1(b) give the spectral positions and maximum gain values predicted by Eqs. (7) and (6) in a fiber which longitudinal evolution of the dispersion is represented in Fig. 1(a) while the black solid line corresponds to the gain obtained from numerics. As can be seen, an excellent agreement is achieved between our model and the simulations. These numerical simulations confirm the validity of our assumptions and the accuracy of our analytical model. This analytical tool will then be useful to investigate the dynamics of MI in amplitude modulated DOFs. For example, the evolution of the gain of the first sidelobe along the fiber calculated using our model is depicted in Fig. 1(c). It shows that the average gain is exponential with oscillations at the two different periods of the dispersion respectively. This result is analogous to the one described in [10]. The evolution of the gain spectrum along the fiber (Media 1) shows that the splitting process is clearly established after a length of propagation equal or superior to the modulation period.

3. Impact of the ratio oscillation period / modulation period

To get more insight into the MI process in amplitude modulated fibers, we investigate the gain spectrum for various ratios Z_1/Z_2. To this purpose, we simulated the gain spectrum of 150 m long fibers with modulation periods Z_2 varying from the infinite (limit-case of the basic oscillating fiber) to the oscillation period Z_1 which is kept constant and equal to 7.5 m. It is worth noting that we do not integrate the NLSE because it would be very time consuming. Instead,

#228256 - $15.00 USD Received 20 Nov 2014; revised 9 Jan 2015; accepted 13 Jan 2015; published 9 Feb 2015

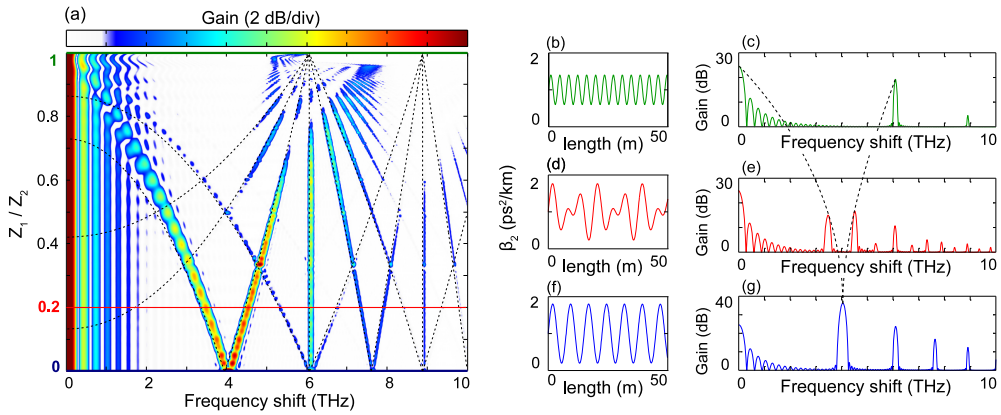

Fig. 2. (a) Gain spectrum in amplitude modulated fibers as a function of the Z_1/Z_2 ratio (Z_1 is fixed and equal to 7.5 m, Z_2 varies from ∞ to Z_1). The dotted lines represent the predicted positions of the sidelobes maximum. Cross-sections of this figure along with sections of the corresponding dispersion profiles are presented for different ratios: (f,g) simply oscillating fiber ($Z_1/Z_2 = 0$), (d,e) amplitude modulated fiber ($Z_1/Z_2 = 0.2$) and (b,c) modulation and oscillation periods are equal ($Z_1/Z_2 = 1$). Same parameters as in Fig. 1.

as we assumed that the pump is not depleted and that its power remains larger than both signal and idler powers, we used a simplified model based on the numerical integration of the basic four coupled equations used to described fiber optical parametric amplifiers composed of multi-section fibers [17]. We adapted it to our configuration by considering that our fiber is composed of many short sections of uniform fibers (typically $\Delta z = 10$ cm). It has the great convenience to be extremely fast compared to a full integration of the NLSE. We checked its accuracy by using the NLSE for the range of parameters we are using. The results are plotted as a 2D map in Fig. 2(a) where the evolution of the MI spectrum is represented as a function of the Z_1/Z_2 ratio. It reveals a complex behaviour with the appearance of new sidelobes compared to the simple sinusoidal modulation format (bottom of the figure). More precisely, all these original sidelobes split into multiple ones of lower gain when the modulation period decreases. In particular, the figure clearly shows that the first (second) sidelobe splits into 2 (3) sidelobes even with a modulation period as long as 75 m ($Z_1/Z_2 = 0.1$). For $Z_1/Z_2 = 0.2$ the gain spectrum is composed of 11 sidelobes (Figure 2(e)) instead of 4 without amplitude modulation of the dispersion (Figure 2(g)). All these observations are in excellent agreement with the predictions of our model (Equation (7)) which are superimposed in dashed lines in Fig. 2(a). Finally, we can state that the amplitude modulation of the dispersion dramatically modifies the modulation instability gain spectrum with the generation of new sidelobes which positions depend on the ratio Z_1/Z_2. This sideband spliting is due to the amplitude modulation of the GVD, and therefore has a completely different physical origin than the one highlighted in [12], where it is due to the large dispersion oscillation at the pump wavelength.

4. Experiments

In order to experimentally validate these results, we designed an amplitude modulated DOF. We optimised the parameters of the system in order to clearly observe the splitting of the first sidelobe in the MI spectrum. We fabricated an air-silica PCF with an air hole-pitch ratio equal to 0.40 (see Fig. 3(d)). Modulation of the dispersion in such fibers is achieved by mean of a modulation of their diameter. The parameters for the fiber are the following: total fiber length:

#228256 - $15.00 USD Received 20 Nov 2014; revised 9 Jan 2015; accepted 13 Jan 2015; published 9 Feb 2015

150 m, $Z_1 = 7.5$ m, $Z_2 = 45$ m ($Z_1/Z_2 = 1/6$), amplitude modulation of the diameter: 7.5 % of the average diameter ($\beta_2^A = 2.1$ ps^2/km), $\alpha_{dB} = 8$ dB/km. We also drawn a basic sinusoidally oscillating fiber with the same parameters as a reference fiber to clearly highlight the impact of the amplitude modulation. Figures 3(b) and 3(c) show both the diameter and dispersion profiles (calculated from [18]) of the reference fiber and of the amplitude modulated fiber respectively for a pump wavelength $\lambda_p = 1057.5$ nm.

A quasi-continuous wave pump beam has been used in these experiments. It is composed of an intensity modulated tunable laser, amplified and filtered to generate 2 ns pulses at a repetition rate of 1 MHz. We checked that the pulses duration was short enough in order to avoid stimulated Brillouin scattering. The polarization of the pump light has been aligned along one of the neutral axes of the fiber to limit our investigations to a scalar configuration. The overall setup is illustrated in Fig. 3(a). Optical spectra recorded in both fibers for a pump wavelength $\lambda_p = 1057.5$ nm are plotted in Fig. 3(e). As expected, multiple sidelobes appear on both sides of the pump in the reference fiber (blue dotted line). For the sake of clarity we limit the wavelength span to only two pairs of sidelobes but six were recorded as can be seen in the inset of Fig. 3(e). In the amplitude modulated DOF (Figure 3(c)), two new sidelobes surround the original one (red solide line). To confirm their origin, we estimated their position by using our analytical model. The experimental positions of the first two sidelobes in the reference fiber let us estimate the values of the average dispersion β_2 and of the nonlinear term $2\gamma P_p$ thanks to the quasi-phase matching relation (1) of [9]. Based on these values, we were able to calculate the detunings for the splitted sidelobes when adding the amplitude modulation of the dispersion using our analytical model. These predicted positions (red arrows) fit very well with the experimental results which confirms their origin.

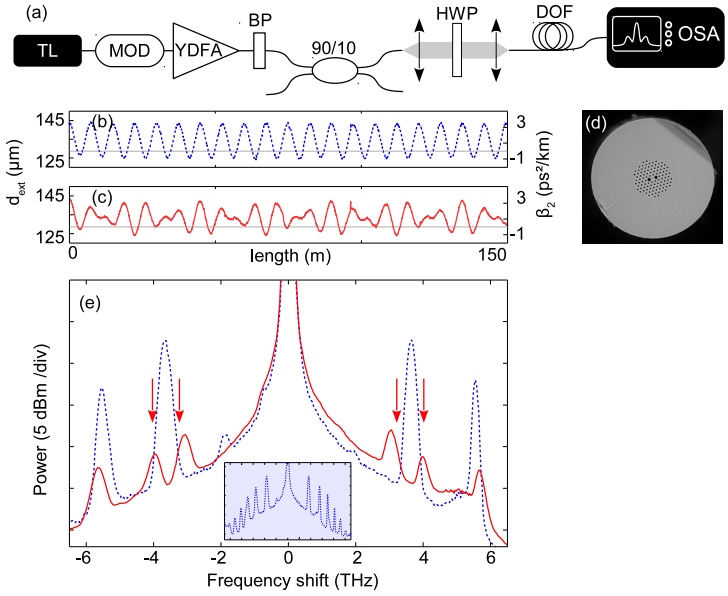

Fig. 3. (a) Experimental setup for the observation of modulation instability. External diameter and dispersion profile of (b) the reference oscillating fiber (c) the amplitude modulated fiber (dispersion scale is calculated for $\lambda_p = 1057.5$ nm). (d) Transverse profile of the PCF. (e) Experimental spectra out of the reference fiber (blue dotted line) and the amplitude modulated fiber (solid red line). The red arrows point out the predicted positions of the first two sidelobes in the amplitude modulated fiber. Inset is the full-span spectrum in the reference fiber exhibiting multiple sidelobes. $P_p = 15$ W, $\gamma = 7.5$ W$^{-1}\cdot$ km^{-1}, $\beta_2 = 1.2$ ps^2/km.

#228256 - $15.00 USD Received 20 Nov 2014; revised 9 Jan 2015; accepted 13 Jan 2015; published 9 Feb 2015

5. Conclusion

We reported the first theoretical, numerical and experimental investigation of the modulation instability process in amplitude modulated dispersion oscillating fibers. We developed an analytical model based on a simple truncated three-wave model that allowed us to obtain an expression for the parametric gain as well as the quasi-phase matching relation. It allows to predict the gain and the position of the new and unexpected modulation instability sidelobes generated in such fibers, with an excellent agreement with numerical simulations. We showed that the amplitude modulation of a sinusoidally varying dispersion fiber leads to the splitting of the original quasi-phase matched sidelobes into many ones, whose position and gain depend on the ratio between the short and the long period of oscillation. Finally, these results have been confirmed experimentally with an excellent agreement with our analytical predictions. This confirms the accuracy and the robustness of our model which can then be viewed as a useful tool in the analysis and the design of such fibers.

Acknowledgments

This work was partly supported by the Agence Nationale de la Recherche through the ANR TOPWAVE and FOPAFE projects, the Labex CEMPI and Equipex FLUX through the ”Programme Investissements d’Avenir”, by the French Ministry of Higher Education and Research, the Nord-Pas de Calais Regional Council and Fonds Européen de Développement Économique Régional (FEDER) through the ”Contrat de Projets État Région (CPER) 2007-2013” and the ”Campus Intelligence Ambiante (CIA)”.